Cold Regions Science and Technology, 6 (1982) 1–10
Elsevier Scientific Publishing Company, Amsterdam – Printed in The Netherlands

SENSITIVITY OF A FROST HEAVE MODEL TO THE METHOD OF NUMERICAL SIMULATION

T.V. Hromadka II, G.L. Guymon
University of California, Irvine, CA 92717 (U.S.A.)

and R.L. Berg
U.S. Army Cold Regions Research and Engineering Laboratory, Hanover, NH 03755 (U.S.A.)

(Received January 23, 1981; accepted in revised form December 22, 1981)

ABSTRACT

A unifying numerical method is developed for solution of frost heave in a vertical freezing column of soil. Within one general computer code a single unifying parameter can be preselected to employ the commonly used Galerkin finite element, subdomain weighted residual, or finite difference methods as well as several other methods developed from the Alternation Theorem. Comparing results from the various numerical techniques in the computation of frost heave to measured frost heave in a laboratory column indicates there is little advantage of one numerical technique over another. One numerical technique, the subdomain method, was used to investigate discretization errors. The model is relatively insensitive to spatial discretization but is significantly sensitive to temporal discretization. The primary reason for this is that an updating procedure, rather than a more accurate iterative procedure, is used to evaluate nonlinear parameters that arise in the moisture transport and heat transport equations.

INTRODUCTION

Guymon et al. (1980) and Hopke (1980) review much of the recent effort to develop comprehensive mathematical models of frost heave. These models can generally be classed as conceptual (or deterministic) models which are developed from physics-based knowledge or assumptions. Generally, most modeling efforts include a simultaneous computation of heat and moisture transport in a freezing soil. Models, however, differ significantly in the manner in which latent heat effects are estimated and in the manner in which ice segregation is assumed to occur. The more advanced efforts to model frost heave have demonstrated that numerical modeling is a feasible tool for analysis of frost heave.

This paper will examine the choice of a numerical analog of the conceptual physics-based equations used in a particular model, i.e. the model investigated by Guymon et al. (1980) will be used as a test case. In order systematically to carry out this purpose, a unifying numerical analog is developed so that appropriate comparisons between numerical methods can be made using identical computer code. Because most models presented in the literature assume the same flow equations, the results presented here are generally applicable. The unifying numerical method that will be used is the nodal domain integration method which represents the subdomain integration method and the common Galerkin finite element and finite difference methods by the specification of a single constant parameter in the resulting spatial discretization matrix system. The nodal domain integration method has been developed for linearized one-

0165-232X/82/0000–0000/$02.75

NUMERICAL MODELING APPROACH

In this section, the nodal domain integration numerical method is briefly reviewed for the reader's convenience. By using the subdomain version of the weighted residuals method defined on subsets of a finite element discretization (nodal domains), an element matrix system is derived similar to the element matrix system developed for a Galerkin finite element analog. The nodal domain integration element matrix system is found to be a function of a single parameter where the Galerkin finite element, subdomain integration, and finite difference methods are represented as special cases. Consequently, the development of a numerical model based on the nodal domain integration method also results in a numerical model based on the more popular Galerkin finite element, subdomain integration, and finite difference methods:

$$A(C) = f; \quad x \in \Omega, \Omega \equiv \Omega \cup \Gamma \tag{1}$$

with boundary condition types of Dirichlet or Neumann specified on boundary Γ. An n-nodal point distribution can be defined on Ω with arbitrary density (Fig. 1) such that an approximation $\hat{C}$ for C is defined in Ω by

$$\hat{C} = \sum_{j=1}^{n} N_j(x) C_j; \quad x \in \Omega \tag{2}$$

where $N_j(x)$ are the usual linearly independent global shape functions (Zienkiewicz, 1977) and C_j are values of the state variable, C, at nodal points j.

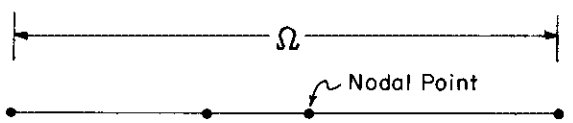

Fig. 1. Nodal point distribution in a one-dimensional domain.

In eqn. (2) it is assumed that

$$\lim_{n\to\infty} \hat{C} = \lim_{\max\|x_j, x_k\|\to\infty} \hat{C} = C, \quad x \in \Omega \tag{3}$$

A cover of Ω is defined by

$$\Omega = \bigcup_{j=1}^{n} R_j \tag{4}$$

where a closed connected subset R_j is defined for each nodal point j such that

$$x_j \in R_j; \quad x_j \notin R_k, \; j \neq k \tag{5}$$

and

$$R_j = R_j \cup B_j \tag{6}$$

where x_j is the spatial coordinate of node j, and B_j is the boundary of subdomain R_j. It is also assumed that

$$R_j \cap R_k = B_j \cap B_k \tag{7}$$

The subdomain version of the finite element method of weighted residuals approximates eqn. (1) on Ω by solving the n equations

$$\int_{\Omega} (A(C) - f) w_j \, dx = 0 \tag{8}$$

where

$$w_j = \begin{cases} 1, & x \in R_j \\ 0, & x \notin R_j \end{cases} \tag{9}$$

A second cover of Ω is given by the usual finite element discretization

$$\Omega = \cup \Omega^e \tag{10}$$

where Ω^e is the closure of finite element and its boundary Γ^e. A set of nodal domains Ω_j^e is defined for each finite element Ω^e by

$$\Omega_j^e = \Omega^e \cap R_j, \quad j \in S_e \tag{11}$$

where S_e is the set of nodal point numbers defined by

$$S_e = \{j \,|\, \Omega^e \cap \Omega_j^e \neq \{\emptyset\}\} \tag{12}$$

That is, S_e is the nodal point number associated with Ω_e. The subdomain integration numerical model of eqn. (8) can be rewritten in the terms of the subdomain cover of Ω by

$$\int_{\Omega} (A(C) - f) w_j \, dx = \int_{R_j} (A(C) - f) \, dx \tag{13}$$

With respect to the finite element discretization of Ω

$$\int_{R_j} (A(C) - f) \, dx = \int_{R_j \cap \Omega} (A(C) - f) \, dx \tag{14}$$

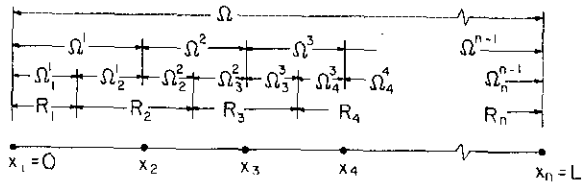

Fig. 2. Nodal domain cover.

For the assumed finite element discretization of Ω, the element matrix system for the finite element Ω^e is given from eqn. (18) as

$$\left\{k_1 \frac{\partial C}{\partial x}\right\}\Big|_{\Gamma_j^e - \Gamma_j^e \cap \Gamma^e} - \{k_2 C\}|_{\Gamma_j^e \cap \Gamma^e} - \{k_2 C\}|_{\Gamma_j^e - \Gamma_j^e \cap \Gamma^e} = \left\{ \int_{\Omega_j^e} k_3 \frac{\partial C}{\partial t}\, dx \right\}, \quad j \in S_e \tag{22}$$

where for an interior finite element ($e \neq 1, n-1$), $S_e = \{e, e+1\}$. Thus, eqn. (22) can be rewritten for an interior Ω^e and an assumed linear trial function, $\bar{C}$, on Ω^e

$$\begin{bmatrix} \left(k_1 \frac{\partial \bar{C}}{\partial x}\right)\Big|_{(x_e + x_{e+1})/2} \\ -\left(k_1 \frac{\partial \bar{C}}{\partial x}\right)\Big|_{(x_e + x_{e+1})/2} \end{bmatrix} - \begin{bmatrix} (k_2 \bar{C})|_{(x_e + x_{e+1})/2} \\ -(k_2 \bar{C})|_{(x_e + x_{e+1})/2} \end{bmatrix} = \begin{bmatrix} \int_{\Omega_e^e} k_3 \frac{\partial \bar{C}}{\partial t}\, dx \\ \int_{\Omega_e^e} k_3 \frac{\partial \bar{C}}{\partial t}\, dx \end{bmatrix} \tag{23}$$

where the second term of eqn. (22) cancels due to neighboring finite elements. Hromadka and Guymon (1981) show that for a first-order polynomial trial function $\bar{C}$ for the state variable C in each finite element, and for the assumed definitions of the subdomain and finite element discretization of problem domain Ω, the Galerkin finite element, subdomain integration, and finite difference numerical analogs can be represented by a single element matrix system similar to eqn. (23) for finite element Ω^e

$$-\frac{k_1}{l_e}\begin{bmatrix} 1 & -1 \\ -1 & 1 \end{bmatrix}\begin{Bmatrix} C_e \\ C_{e+1} \end{Bmatrix} + \frac{k_2}{2}\begin{bmatrix} 1 & -1 \\ 1 & -1 \end{bmatrix}\begin{Bmatrix} C_e \\ C_{e+1} \end{Bmatrix} = \frac{l_e k_3}{2(\eta+1)}\begin{bmatrix} \eta & 1 \\ 1 & \eta \end{bmatrix}\begin{Bmatrix} \partial C_e/\partial t \\ \partial C_{e+1}/\partial t \end{Bmatrix} \tag{24}$$

where $\eta = (2, 3, \infty)$ gives the Galerkin finite element, subdomain integration, and finite difference models, respectively. In eqn. (24) the nonlinear parameters (k_1, k_2, k_3) are assumed constant for a small duration of time Δt, l_e is the length of finite element Ω^e, and C_e is the nodal point value. Generally, convection is assumed to be negligible in eqn. (24) and the k_2 parameter is set to zero. For this study, however, convection is maintained but approximated as a constant for a small duration of time Δt.

From eqn. (24), a single model can be developed which can represent the Galerkin finite element, subdomain integration, and finite difference methods for approximating the governing heat and soil water flow equations. The method of linearizing the governing flow equations is to assume all nonlinear parameters to be constant during a small timestep Δt. From the above, the element matrix system used to approximate the governing flow equations in finite element Ω^e becomes

$$-\frac{k_1}{l_e}\begin{bmatrix} 1 & -1 \\ -1 & 1 \end{bmatrix}\begin{Bmatrix} C_e \\ C_{e+1} \end{Bmatrix} = \frac{l_e k_3}{2(\eta+1)}\begin{bmatrix} \eta & 1 \\ 1 & \eta \end{bmatrix}\begin{Bmatrix} \partial C_e/\partial t \\ \partial C_{e+1}/\partial t \end{Bmatrix} - \frac{k_2}{2}\begin{bmatrix} 1 & -1 \\ 1 & -1 \end{bmatrix}\begin{Bmatrix} \bar{C}_e \\ \bar{C}_{e+1} \end{Bmatrix} \tag{25}$$

where $\{\bar{C}_e, \bar{C}_{e+1}\}$ are temporally averaged nodal values during timestep Δt. The Crank–Nicolson time advancement approximation can be used to integrate eqn. (25) with respect to time giving

$$(H(\eta) + \tfrac{1}{2}\Delta t\, G)\, C^{(k+1)\Delta t} = (H(\eta) - \tfrac{1}{2}\Delta t\, G)\, C^{k\Delta t} - \beta \Delta t \tag{26}$$

where C is the vector of nodal point values at time $(k+1)\Delta t$ and $k\Delta t$; β is an assumed constant value for convection in Ω^e during timestep Δt; and the element matrices are given by

$$G = \frac{k_1}{l_e}\begin{bmatrix} 1 & -1 \\ -1 & 1 \end{bmatrix} \tag{27}$$

where (i) represents the ith-order temporal partial differential operator. Then

$$\left\{ k_1 \frac{\partial \hat{C}}{\partial x} \right\} \Big|_{B_j} = \left\{ \sum_{i=0}^{\infty} A^{(i)}(k\Delta t) \frac{\epsilon^i}{i!} \frac{\partial \bar{C}}{\partial x} \right\} \Big|_{B_j} \quad (35)$$

A function $\eta(t)$ is defined by

$$\int_{R_j} \hat{C} \mathrm{d}x = \frac{\bar{l}}{2[\eta(t)+1]} \{C_{j-1} + 2C_j\,\eta(t) + C_{j+1}\} \quad (36)$$

where $\bar{l} = \|R_j\|$, and

$$\eta(t) \neq -1 \quad (37)$$

The value of $\eta=3$ in eqn. (36) corresponds to a first-order polynomial $\hat{C}$ function subdomain approximation for C, whereas $\eta(t) = 2$ corresponds to a Galerkin finite element model, and $\eta(t) = \infty$ determines a finite difference model.

The $\bar{C}$ approximator is also defined to have the property

$$\int_{R_j} \bar{C}\ \mathrm{d}x \equiv \int_{R_j} \hat{C}\,\mathrm{d}x, \quad \eta(t) \neq -1 \quad (38)$$

Substituting eqns. (35) and (36) into eqn. (22) gives the modeling statement (for convection β quasi-constant during timestep Δt)

$$\int_{\Delta t} \left\{ \sum_{i=0}^{\infty} A^{(i)}(k\Delta t) \frac{\epsilon^i}{i!} \frac{\partial \bar{C}}{\partial x} \right\} \Big|_{B_j} \mathrm{d}\epsilon$$

$$= k_3(k\Delta t+\Delta t) \frac{\bar{l}[C^*_{j-1} + 2C^*_j \eta(k\Delta t+\Delta t) + C^*_{j+1}]}{2[\eta(k\Delta t+\Delta t)+1]}$$

$$- k_3(k\Delta t) \frac{\bar{l}[C'_{j-1} + 2C'_j\,\eta(k\Delta t) + C'_{j+1}]}{2[\eta(k\Delta t)+1]} + \beta\Delta t \quad (39)$$

where $C^*_j = C_j(k\Delta t+\Delta t)$; $C'_j = C_j(k\Delta t)$; and where k_3 is assumed uniform in R_j, and

$$\eta(k\Delta t+\epsilon) = \sum_{i=0}^{\infty} \eta^{(i)}(k\Delta t) \frac{\epsilon^i}{i!}; \quad 0 \leqslant \epsilon \leqslant \Delta t \quad (40)$$

Integrating the conduction term in eqn. (39) on Ω^e gives

$$\left.\begin{aligned} \bar{\bar{A}}(\lambda) &= \frac{1}{l_e} \sum_{i=0} \frac{A^{(i)}(\lambda)(\Delta t)^{i+1}}{i!(i+2)} \\ \bar{A}(\lambda) &= \frac{1}{l_e} \sum_{i=0}^{\infty} \frac{A^{(i)}(\lambda)(\Delta t)^{i+1}}{(i+2)!} \end{aligned}\right\} \lambda \in B_j,\ \lambda \in \hat{\Omega}_e \quad (41)$$

The nodal domain integration element matrix system similar to eqn. (26) is given by

$$(\bar{\bar{H}} + \bar{\bar{G}})\,\{C\}^{(k+1)\Delta t} = (\bar{H} - \bar{G})\,\{C\}^{k\Delta t} - \beta\Delta t \quad (42)$$

where

$$\left.\begin{aligned} \bar{\bar{G}} &= \bar{\bar{A}}(\lambda) \begin{bmatrix} 1 & -1 \\ -1 & 1 \end{bmatrix} \\ \bar{G} &= \bar{A}(\lambda) \begin{bmatrix} 1 & -1 \\ -1 & 1 \end{bmatrix} \\ \bar{\bar{H}}(\eta) &= \frac{l_e}{2(\bar{\bar{\eta}}+1)} \begin{bmatrix} \bar{\bar{\eta}} & 1 \\ 1 & \bar{\bar{\eta}} \end{bmatrix} \\ \bar{H}(\eta) &= \frac{l_e}{2(\bar{\eta}+1)} \begin{bmatrix} \bar{\eta} & 1 \\ 1 & \bar{\eta} \end{bmatrix} \end{aligned}\right\}$$

and where $\bar{\bar{\eta}} = \eta(k\Delta t+\Delta t)$, $\bar{\eta} = \eta(k\Delta t)$, $l_e = \|\Omega^e\|$, and λ is the midpoint of Ω^e.

RESULTS

The numerical models of eqns. (26) and (42) were used to solve the governing heat and soil water flow equations as used in the Guymon et al. (1980) *frost heave model*. Since the only variation of the numerical model required to determine a Galerkin finite element, subdomain integration, finite difference, or nodal domain integration analog is the adjustment of the η term in eqn. (26), a single computer code may be used. As a result, variability normally inherent between computer programs is entirely eliminated, giving a precise comparison of numerical methods. A Fairbanks silt vertical soil freezing column test as described in Berg et al. (1980) is used as the test case for determining the sensitivity of the frost heave model to the method of numerical simulation. The laboratory test used is for a soil column freezing case in which frost penetrated

the choice of numerical model for the one-dimensional problem considered here are much less than errors introduced by parameter uncertainty (Guymon et al., 1981) and by boundary condition uncertainty.

It should be noted that Table 3 lists the numerical approximation results for the largest timestep size used in this sensitivity study. A smaller timestep gives significantly better approximation results as is indicated in Table 3 for a timestep of 0.5 h (for η=3). This increase in approximation accuracy is mainly due to the better modeling of the nonlinear parameters used in the frost heave model.

CONCLUSIONS

A frost heave model is examined in an effort to determine the sensitivity of predicted frost heave values to the choice of numerical method used to solve the governing heat and soil water flow equations. A computer code based on the nodal domain integration method accommodates several other numerical analogs by the specification of a single constant parameter η in the resulting element matrix contributions; consequently, sensitivity of the frost heave model to the method of numerical simulation can be determined by the variation of the single parameter η.

From the simulation results, the Guymon et al. frost heave model shows negligible sensitivity to the numerical approach used to solve the governing flow equations. Although sensitivity is observed initially for a large timestep choice, all frost heave evolution curves are found to merge at the end of the 25 day simulation. Since freezing soil problems are generally subjected to freezing temperatures for durations in excess of 25 days, it is concluded that negligible sensitivity occurs due to the numerical approach chosen to model the heat and soil water flow equations in the considered frost heave model. One numerical method is as good as another. Variations between the variously proposed models (e.g. as reviewed by Hopke, 1980) will primarily depend upon efficiency of code and user orientated features; there seems to be little point in debating the virtues of a particular numerical method. We conclude that modeling errors that can be associated with model choice (eqn. (1)) will primarily be related for the choice of governing equations and ancillary assumptions used in a model. Whether we can definitely isolate errors associated with the choice of such equations and assumptions will depend on our ability to isolate the other errors we have identified.

The type of model investigated by Guymon et al. (1980) shows minor sensitivity to spatial discretization while there is significant sensitivity to temporal discretization. This is largely due to the nonlinear nature of the problem we are dealing with and the updating method of adjusting nonlinear problems. True iterative techniques would probably show less sensitivity to temporal discretization but would require considerably more solution time.

Our results suggest that solutions are reasonably bounded. Consequently, the fact that our model does not account for all processes occurring at the freezing front is not a significant concern from an engineering applicability criterion. Provided boundedness can be defined, the model can be employed with a certain level of confidence in the statistical sense.

NOTATION

$A(\ )$	partial differential operator
C_m	volumetric heat capacity of soil–water–ice mixture
C_w	volumetric heat capacity of water
K_H	Darcy hydraulic conductivity
K_T	thermal conductivity of soil–water–ice mixture
n	number of nodal points
$N_j(x)$	shape function
H	finite element capacitance matrix
G	finite element stiffness matrix
t	time
Δt	timestep of numerical temporal integration
T	temperature of soil–water–ice mixture
C	state variable, ϕ or T
v	Darcy flux
x	spatial coordinate
ϕ	total hydraulic head, $\phi = \psi - x$ (x measured downwards)
ψ	pore water pressure head
Ω	global domain of definition
Ω^e	finite element domain
R_j	subdomain
Ω_j^e	nodal domain

Γ boundary of global domain
Γ^e finite element boundary
Γ_j^e nodal domain boundary
B_j subdomain boundary
β quasi-constant value of convection term during timestep Δt

T_f freezing point depression of water
T_u soil surface temperature boundary condition
T_L column bottom temperature boundary condition

Ψ_L column bottom pore pressure boundary condition
Ψ_o surcharge plus overburden pressure expressed as hydraulic head
θ_o porosity
θ_n volumetric unfrozen water content factor
θ_u volumetric unfrozen water content
θ_i volumetric ice content
ρ_i density of ice
ρ_w density of liquid water
L latent heat of fusion

K_i thermal conductivity of ice
K_w thermal conductivity of water
K_s thermal conductivity of soil
C_m volumetric heat capacity of soil–water–ice mixture
C_i volumetric heat capacity of ice
C_w volumetric heat capacity of water
C_s volumetric heat capacity of soil
l length of finite volume of soil

k timestep increment number, $k \geqslant 0$
k_i nonlinear operator parameters, $i = 1, 2, 3$
$\bar{l}$ length of subdomain
l_e length of finite element
C state variable
$\hat{C}$ higher-order trial function
$\bar{C}$ linear polynomial trial function

C_j nodal point values of state variable C at node j
C_j^* $C_j(k\Delta t+\Delta t)$
C_j' $C_j(k\Delta t)$

ACKNOWLEDGEMENTS

This research was supported by the U.S. Army Research Office (Grant No. DAAG29-79-C-0080) and by the U.S. Army, Cold Regions Research and Engineering Laboratory, Hanover, New Hampshire, where the second author was on sabbatical leave during 1980–81.

REFERENCES

Berg, R.L., Ingersoll, J. and Guymon, G.L. (1980), Frost heave in an instrumented soil column, Cold Regions Sci. Technol., 3 (2&3): 211–221.

Cheney, E.W. (1966), Introduction to Approximation Theory, McGraw-Hill.

Guymon, G.L., Hromadka II, T.V. and Berg, R.L. (1980), A one dimensional frost heave model based upon simulation of simultaneous heat and water flux, Cold Regions Sci. Technol., 3 (2&3): 253–262.

Guymon, G.L., Harr, M.E., Berg, R.L. and Hromadka II, T.V. (1981), A probabilistic–deterministic analysis of one-dimensional ice segregation in a freezing soil column, Cold Regions Sci. Technol., 5 (2): 127.

Hopke, S.S. (1980), A model for frost heave including overburden, Cold Regions Sci. Technol., 3 (2&3): 111–127.

Hromadka II, T.V. and Guymon, G.L. (1980), Some effects of linearizing the unsaturated soil-moisture transfer diffusion model, Water Resources Res., 16: 633–640.

Hromadka II, T.V. and Guymon, G.L. (1981), Improved linear shape function model of soil moisture transport, Water Resources Res., 17 (3): 504–521.

Hromadka II, T.V. and Guymon, G.L. (1982), Nodal domain integration model of one dimensional advection–diffusion, Adv. Water Resources, 5: 9–16.

Hromadka II, T.V., Guymon, G.L. and Pardoen, G.C. (1981), Nodal domain integration model of unsaturated two-dimensional soil water flow: Development, 17(5): 1425–1430.

Zienkiewicz, O.C. (1977), The Finite Element Method, McGraw-Hill, New York.

at an approximately uniform rate until a depth of 15 cm was reached at about 25 days after initiation of the test. Frost heave proceeded at a more or less uniform rate during this test. During the test all components of the system were in a dynamic state.

Using identical problem initial and boundary conditions, a 25 day duration computer simulation was made varying timestep and element discretization magnitudes as well as varying constant values of η given in Table 2. Values of timesteps used in the temporal numerical integration (Crank–Nicolson time advancement approximation) are Δt = (0.1, 0.2, 0.4, 1.0, 2.0 h). Constant finite element sizes used are $\Delta x \equiv \|\Omega^e\| = (\frac{1}{2}, 1, 1.5, 3.0$ cm). For each combination of $(\Delta x, \Delta t)$ values, constant values of η = (2, 3, 5.9, 7, 11, 10 000) were tested representing a linear trial function Galerkin finite element, subdomain integration, nodal domain integration linear approximation of a sinusoidal and parabola trial function, subdomain integration model of parabola trial function, and finite difference numerical analogs, respectively.

Figure 4 shows the results of varying timestep and spatial discretization using the subdomain method (η=3). Simulated heave is compared to measured heave for a laboratory column and error in percent is computed by taking the difference and dividing by measured heave after 25 days. Similar results to Fig. 4 are obtained for shorter durations of time. As can be seen, there is slight sensitivity to spatial discretization, and marked sensitivity to timestep size for advancing the solution in time. A timestep of about 0.5 h gives the best result. It is important to note that the method proposed by Guymon et al. (1980) uses a simple update procedure to adjust nonlinear parameters rather than a possibly more accurate iteration procedure normally employed with nonlinear equations.

Table 3 compares computed frost heave for a timestep size and update frequency of 2 h and a spatial uniform discretization of 3 cm. Results shown in Table 3 are typical of results obtained using choice of different timesteps and mesh sizes. As can be seen there is initially some sensitivity in the numerical method; however after 10 days, differences between numerical methods are slight. Errors associated with

TABLE 3

Comparison of results for various numerical methods (timestep = 2 h, Δx = 3 cm)

η	Cumulative frost heave for indicated day				
	5	10	15	20	25
2	0.61	2.22	2.85	3.52	4.46
3	0.66	2.26	2.88	3.52	4.46
7	0.72	2.29	2.90	3.49	4.44
11	0.74	2.29	2.90	3.48	4.43
∞	0.77	2.29	2.90	3.46	4.41
Measured	1.6	2.8	3.9	4.4	5.0
timestep = 0.5 h	1.3	2.5	3.4	4.2	5.0

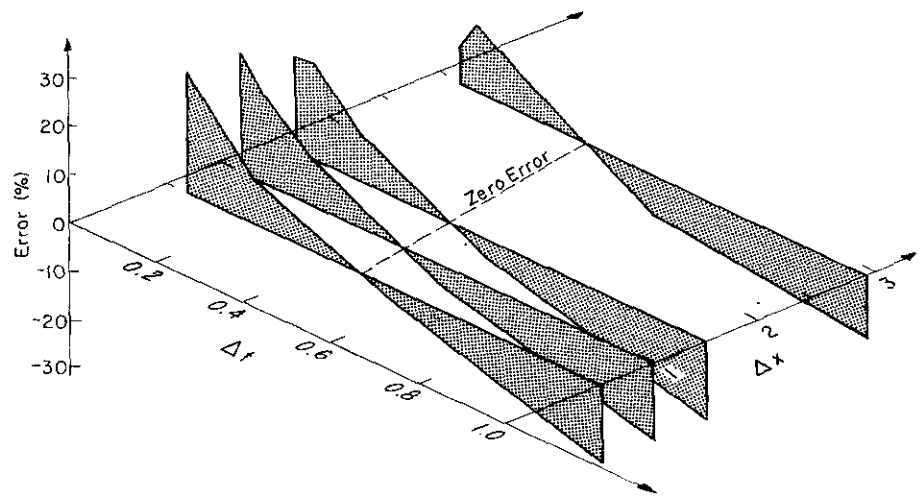

Fig. 4. Frost heave simulation error as a function of spatial and temporal discretization.

$$H(\eta) = \frac{k_3 l_e}{2(\eta+1)} \begin{bmatrix} \eta & 1 \\ 1 & \eta \end{bmatrix} \tag{28}$$

Hromadka and Guymon (1982) also examined two methods of approximating a higher-order or more complex family of trial functions by a linear polynomial trial function. One method used the Alternation Theorem (Cheney, 1966) to determine an optimum linear polynomial estimate of a higher-order approximator. Using an adjusted linear trial function $\bar{C}$ approximation of a higher-order trial function $\hat{C}$ approximation of the state variable C in each finite element Ω^e (Fig. 3), it was shown that the gradient terms due to conduction were given by eqn. (27), but the integrated mass matrix term was given by eqn. (28) with values of η depending on the function definition of $\hat{C}$. For example, given a sinusoidal trial function $\hat{C}$ in each Ω^e, an optimum linear approximation $\bar{C}$ of $\hat{C}$ in Ω^e results in a value of $\eta = 5.9$. For a parabola trial function $\hat{C}$ in Ω^e, eqn. (28) is determined to be given by $\eta = 7$ when $\hat{C}$ is approximated by a linear trial function in each Ω^e. Additionally, by

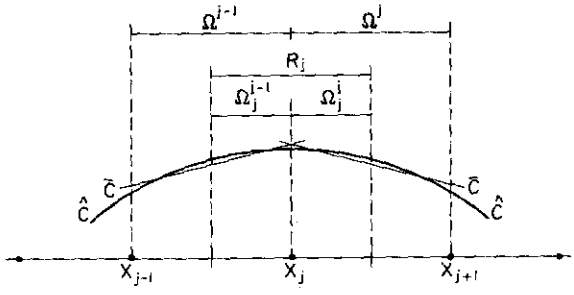

Fig. 3. Adjusted linear trial function using the alternation theorem.

TABLE 2

Nodal domain integration η-factor representations

η factor	Numerical method
2	Galerkin finite element (linear trial function)
3	Subdomain (linear trial function)
5.9	Linear trial function approximation of sine function
7	Linear trial function approximation of parabolic function
11	Subdomain (second-order polynomial trial function)
∞ (e.g. 10 000)	Finite difference

assuming $\hat{C}$ to be given by second-order polynomials in each subdomain R_j, integration of the governing flow equations results in $\eta = 11$. The various submethods of the nodal domain integration concept (using the Alternation Theorem) derived to date are listed in Table 2.

A second method of approximating a higher-order or more complex family of trial functions $\hat{C}$ for the state variable C is by use of correction functions for both the integration and differentiation of C in each subdomain R_j. This approach was found to give the best numerical accuracy for the problems tested, and resulted in a numerical statement similar to eqn. (26) but with η a function of time, and variable between finite elements. This approach is reviewed in the following.

Let $\bar{C}$ be a linear approximation function of a higher-order approximation $\hat{C}$ of C in an interior subdomain R_j where the spatial gradients of $\bar{C}$ on B_j are defined by

$$\left\{\frac{\partial \bar{C}}{\partial x}\right\} \Big|_{B_j} \equiv \frac{(C_{j+1} - C_j)}{l_j} - \frac{(C_j - C_{j-1})}{l_{j-1}},$$

$$l_j \equiv \|\Omega^j\| \tag{29}$$

A spatial gradient adjustment function $h(x,t)$ is defined by

$$h(x,t) \equiv \begin{cases} \dfrac{\partial \hat{C}}{\partial x} \Big/ \dfrac{\partial \bar{C}}{\partial x}\ ; & 0 < h < \infty \\ 1 \quad ; & \text{otherwise} \end{cases} \tag{30}$$

It is assumed that

$$k_1 \frac{\partial \hat{C}}{\partial x} = k_1 h \frac{\partial \bar{C}}{\partial x} \tag{31}$$

where

$$\left\{k_1 \frac{\partial \hat{C}}{\partial x}\right\} \Big|_{B_j} = \left\{k_1 h \frac{\partial \bar{C}}{\partial x}\right\} \Big|_{B_j} \tag{32}$$

On B_j, define

$$k_1 h = A(t); \quad k\Delta t \leqslant t \leqslant (k+1)\Delta t \tag{33}$$

such that

$$A(k\Delta t + \epsilon) = \sum_{i=0}^{\infty} A^{(i)}(k\Delta t) \frac{\epsilon^i}{i!}; \quad 0 \leqslant \epsilon \leqslant \Delta t \tag{34}$$

where for each finite element domain Ω^e

$$\int_{\Omega^e \cap R_j} A(C) - f)\,dx = \int_{\Omega_j^e} (A(C) - f)\,dx \qquad (15)$$

From eqn. (15), the subdomain method of weighted residuals determines an element matrix system for each finite element Ω^e by the integration of the governing equation on each member of the nodal domain cover Ω_j^e. The spatial definition of each nodal domain Ω_j^e depends on the definition of both the finite element and subdomain discretization of Ω, and is therefore somewhat arbitrary. A convenient criterion is to define the nodal domains such that the resulting finite element matrix system is symmetric. This symmetric property is used for the definition of the subdomain cover R_j of Ω in the following model development of a one-dimensional advection diffusion type process. Extension of the one-dimensional nodal domain integration procedure to two-dimensional problems are contained in Hromadka et al. (1981).

The governing heat and soil water flow equations can be written in the operator relationship

$$A(C) - f = \frac{\partial}{\partial x}\left[k_1 \frac{\partial C}{\partial x}\right] - \frac{\partial}{\partial x}[k_2 C] - k_3 \frac{\partial C}{\partial t}; \quad x \in \Omega \qquad (16)$$

where all parameters are assumed to be continuous in Ω, and where for the heat flow process k_1 = thermal conductivity, $k_2 = C_\omega v$, $k_3 = C_m$, and C = temperature, T. For the soil water flow equation $k_1 = K_H$, $k_2 = 0$, $k_3 = \partial\theta/\partial\psi$, and $C = \phi$. The ice content terms of both flow processes are not needed in eqn. (16) due to the isothermal phase change approximation used by Guymon et al. (1980). Therefore, eqn. (16) is solved for heat and soil water flow processes during a small timestep Δt; then, the computed values of unfrozen water content, ice content and temperature are recalculated to accommodate isothermal phase change of available soil water. Substituting the operator relationship of eqn. (16) into the integration statement of eqn. (15) gives an element matrix system for finite element Ω^e

$$\left\{\int_{\Omega_j^e}\left(\frac{\partial}{\partial x}\left[k_1 \frac{\partial C}{\partial x}\right] - \frac{\partial}{\partial x}[k_2 C] - k_3 \frac{\partial C}{\partial t}\right)dx\right\} = \{0\}; \quad j \in S_e \qquad (17)$$

Expanding eqn. (17) gives the element matrix components for the conduction, convection, and mass terms of the operator relationship

$$\left\{k_1 \frac{\partial C}{\partial x}\bigg|_{\Gamma_j^e \cap \Gamma^e}\right\} - \{k_2 C|_{\Gamma_j^e \cap \Gamma^e}\} + \left\{k_1 \frac{\partial C}{\partial x} - k_2 C\bigg|_{\Gamma_j^e - \Gamma_j^e \cap \Gamma^e}\right\} = \left\{\int_{\Omega_j^e} k_3 \frac{\partial C}{\partial t}\,dx\right\}, \quad j \in S_e \qquad (18)$$

The first matrix term of eqn. (18) cancels due to flux contributions from neighboring finite elements or satisfies zero flux (Neumann) boundary conditions on Γ. In order to develop the element matrices for Ω^e from eqn. (18), a definition of a subdomain and finite element discretization of domain Ω is required.

A cover of spatial domain Ω is given by the set of n closed connected subdomains R_j defined by

$$\begin{aligned} R_1 &\equiv \{x|\, 0 = x_1 \leqslant x \leqslant (x_1 + x_2)/2\} \\ R_2 &\equiv \{x|\, (x_1 + x_2)/2 < x \leqslant (x_2 + x_3)/2\} \\ R_n &\equiv \{x|\, (x_{n-1} + x_n)/2 < x \leqslant x_n = L\} \end{aligned} \qquad (19)$$

where x_j is the spatial coordinate associated to nodal point value C_j. In eqn. (19), C_j represents nodal point values of temperature and total hydraulic head for the heat and soil water flow equations, respectively. In the following, the definition of the subdomain discretization of Ω given in eqn. (19) will be shown to result in symmetrical element conduction and element mass matrices.

The finite element discretization of domain Ω is assumed to be composed of one-dimensional elements defined by

$$\begin{aligned} \Omega^1 &\equiv \{x|x_1 \leqslant x \leqslant x_2\} \\ \Omega^2 &\equiv \{x|x_1 \leqslant x \leqslant x_3\} \\ \Omega^{n-1} &\equiv \{x|x_{n-1} \leqslant x \leqslant x_n\} \end{aligned} \qquad (20)$$

The nodal domain cover of global domain Ω is defined by the intersection of the finite element and subdomain covers of Ω (Fig. 2)

$$\begin{aligned} \Omega_1^1 &\equiv \{x|x_1 \leqslant x \leqslant x_1/2\} \\ \Omega_2^1 &\equiv \{x|x_1/2 \leqslant x \leqslant x_2\} \\ \Omega_n^{n-1} &\equiv \{x|(x_{n-1} + x_n)/2 \leqslant x \leqslant x_n\} \end{aligned} \qquad (21)$$

dimensional transport equations (Hromadka and Guymon, 1982) and has been extended to two dimensions using linear trial functions (Hromadka et al., 1981). These references include evaluation of numerical errors when comparing to exact solutions. Hromadka and Guymon (1980) examine some effects of linearizing nonlinear equations. In this paper, the nodal domain integration method is applied to a nonlinear coupled heat and moisture transport problem. The application of nodal domain integration to such problems is a new contribution. Furthermore, the application of numerical solution techniques to the frost heave problem is a rather new endeavor and one aspect of the problem, the choice of numerical technique, deserves examination.

Previously, Guymon et al. (1981) discussed model errors and examined in detail errors associated with parameters of a deterministic model of frost heave. Four arbitrary groups of errors were identified:

1. Model errors including numerical analog errors.
2. Spatial and temporal discretization errors.
3. Boundary and initial condition errors.
4. Parameter errors.

Numerical analog errors may be investigated in simple cases by linearizing a problem and comparing a numerical solution to an analytic or so-called "exact" solution. In the case of our multiparameter model, it is highly nonlinear and heat and moisture transport are coupled through the parameters arising from the conceptual assumptions employed. Furthermore, several ancillary equations are used to estimate parameters and processes involved. The only realistic way of evaluating errors is to compare model output with prototype output. This approach is highly effective in this case where lumped frost heave represents or integrates all the complicated processes occurring in a freezing soil. A set of data obtained in the laboratory for Fairbanks silt is used for comparison with numerical solutions.

A particular deterministic model of one-dimensional frost heave in a vertical saturated or partly saturated soil column is used herein (Guymon et al., 1980). Details of this model will not be repeated here. The modeling concept is shown in Table 1. Symbols used in this table are defined under "Notation". Moisture flow in a partly saturated column toward a freezing frost is assumed to obey continuity and Darcy's law. Sensible heat flow in both the frozen and unfrozen zones is estimated. Complicated processes in the freezing zone are lumped into an assumed isothermal freezing process. This process controls the rate and magnitude of frost heave in the model and integrates all other model processes.

TABLE 1

Deterministic equations for one-dimensional frost heave model

Soil region	Energy state	Liquid moisture transport	Phase change	Sensible heat transport	Ancillary relationships
Surface boundary		$\partial(\psi - x)/\partial x = 0$		$T_u = T(t)$	
Frozen	$T < T_f$ $\psi = \psi(\theta_n) + \delta\psi_o$ $\delta = \begin{cases} 1, \theta_i \geq \theta_o - \theta_n \\ 0, \theta_i < \theta_o - \theta_n \end{cases}$	$\partial(\psi - x)/\partial x = 0 = \nu$	$\frac{\partial \theta_i}{\partial t} = 0$	$\frac{\partial}{\partial x}\{K_T \partial T/\partial x\} = C_m \frac{\partial T}{\partial t}$	$K_H = K(\psi) \times 10^{-E\theta_i}, E\theta_i \geq 1$ $\theta_u = \theta(\psi)$ $\nu = -K_H\, \partial(\psi - x)/\partial x$
Freezing or thawing	$T = T_f$ $\psi(\theta_n) < \psi < 0$	$\frac{\partial \theta_u}{\partial t} = \frac{\partial}{\partial x}[K_H\, \partial(\psi - x)/\partial x] - \frac{\rho_i}{\rho_w}\frac{\partial \theta_i}{\partial t}$	$L\frac{\rho_i}{\rho_w}\frac{\partial \theta_i}{\partial t}$	$+\frac{\partial}{\partial x}[K_T\, \partial T/\partial x] - C_w \nu \frac{\partial T}{\partial x} = C_m \frac{\partial T}{\partial t}$	$C_m = \{C_i\theta_i + C_w\theta_u + C_s(1 - \theta_o)\}/(1+\theta_s)$ $K_T = \{K_i\theta_i + K_w\theta_u + K_s(1 - \theta_o)\}/(1+\theta_s)$
Unfrozen	$T > T_f$ $\psi(\theta_n) < \psi < \psi_L$	$\frac{\partial \theta_u}{\partial t} = \frac{\partial}{\partial x}[K_H \partial(\psi - x)/\partial x]$	$\frac{\partial \theta_i}{\partial t} = 0$	$\frac{\partial}{\partial x}[K_T \partial T/\partial x] - C_w \nu \frac{\partial T}{\partial x} = C_m \frac{\partial T}{\partial t}$	$\nu = \Sigma \theta_s \ell$
Column bottom boundary		$\psi_L = \psi(t)$		$T_L = T(t) > T_f$	